



HAL
open science

Evolution of VIM-1-Producing *Klebsiella pneumoniae* Isolates from a Hospital Outbreak Reveals the Genetic Bases of the Loss of the Urease-Positive Identification Character

Nicolas Cabanel, Isabelle Rosinski-Chupin, Adriana Chiarelli, Tatiana Botin, Marta Tato, Rafael Canton, Philippe Glaser

► **To cite this version:**

Nicolas Cabanel, Isabelle Rosinski-Chupin, Adriana Chiarelli, Tatiana Botin, Marta Tato, et al.. Evolution of VIM-1-Producing *Klebsiella pneumoniae* Isolates from a Hospital Outbreak Reveals the Genetic Bases of the Loss of the Urease-Positive Identification Character. *mSystems*, 2021, 6 (3), pp.e0024421. 10.1128/mSystems.00244-21 . pasteur-03519675

HAL Id: pasteur-03519675

<https://pasteur.hal.science/pasteur-03519675>

Submitted on 10 Jan 2022

HAL is a multi-disciplinary open access archive for the deposit and dissemination of scientific research documents, whether they are published or not. The documents may come from teaching and research institutions in France or abroad, or from public or private research centers.

L'archive ouverte pluridisciplinaire **HAL**, est destinée au dépôt et à la diffusion de documents scientifiques de niveau recherche, publiés ou non, émanant des établissements d'enseignement et de recherche français ou étrangers, des laboratoires publics ou privés.



Distributed under a Creative Commons Attribution 4.0 International License



Evolution of VIM-1-Producing *Klebsiella pneumoniae* Isolates from a Hospital Outbreak Reveals the Genetic Bases of the Loss of the Urease-Positive Identification Character

Nicolas Cabanel,^{a,b} Isabelle Rosinski-Chupin,^{a,b} Adriana Chiarelli,^{a,b,c} Tatiana Botin,^{a,b} Marta Tato,^d  Rafael Canton,^d  Philippe Glaser^{a,b}

^aEERA Unit "Ecology and Evolution of Antibiotics Resistance," Institut Pasteur-Assistance Publique/Hôpitaux de Paris-Université Paris-Saclay, Paris, France

^bUMR CNRS 3525, Paris, France

^cSorbonne Université, Paris, France

^dServicio de Microbiología, Hospital Universitario Ramón y Cajal and Instituto Ramón y Cajal de Investigación Sanitaria (IRYCIS), Madrid, Spain

Isabelle Rosinski-Chupin, Adriana Chiarelli, and Tatiana Botin contributed equally to this work.

ABSTRACT Outbreaks of carbapenemase-producing *Klebsiella pneumoniae* (CPKp) represent a major threat for hospitals. We molecularly characterized the first outbreak of VIM-1-producing *K. pneumoniae* in Spain, which raised fears about the spread of this strain or of the plasmid carrying *bla*_{VIM-1}. Through in-depth genomic analysis of 18 isolates recovered between October 2005 and September 2007, we show that 17 ST39 isolates were clonal, whereas the last isolate had acquired the VIM-1 plasmid from the epidemic clone. The index isolate carried 31 antibiotic resistance genes (ARGs) and was resistant to almost all antibiotics tested. Later isolates further gained mutations in efflux pump regulators *ramR* and *opxR*, deletion of *mgrB* (colistin resistance), and frameshift mutations in *ompK36* (β -lactam resistance) likely selected by antibiotic usage. Comparison with publicly available genome sequences and literature review revealed no sign of dissemination of this CPKp strain. However, the VIM-1 plasmid was found in diverse Enterobacterales species, although restricted to Spain. One isolate became urease negative following IS5075 transposition into *ureC*. Analysis of 9,755 *K. pneumoniae* genomes showed the same *ureC*::IS5075 insertion in 14.1% of the isolates and explained why urease activity is a variable identification trait for *K. pneumoniae*. Transposition into *ureC* results from the similarity of its 3' end and the terminal inverted repeats of Tn21-like transposons, the targets of IS5075 and related insertion sequences (ISs). As these transposons frequently carry ARGs, this might explain the frequent chromosomal invasion by these ISs and *ureC* inactivation in multidrug-resistant isolates.

IMPORTANCE Evolution of multidrug-resistant bacterial pathogens occurs at multiple scales, in the patient, locally in the hospital, or more globally. Some mutations or gene acquisitions, for instance in response to antibiotic treatment, may be restricted to a single patient due to their high fitness cost. However, some events are more general. By analyzing the evolution of a hospital-acquired multidrug-resistant *K. pneumoniae* strain producing the carbapenemase VIM-1, we showed a likely environmental source in the hospital and identified mutations contributing to a further decrease in antibiotic susceptibility. By combining the genomic analysis of this outbreak with literature data and genome sequences available in databases, we showed that the VIM-1 plasmid has been acquired by different Enterobacterales but is endemic only in Spain. We also discovered that urease loss in *K. pneumoniae* results from the specific transposition of an IS element into the *ureC* gene and was more frequent in fluoroquinolone-resistant isolates and those carrying a carbapenemase gene.

Citation Cabanel N, Rosinski-Chupin I, Chiarelli A, Botin T, Tato M, Canton R, Glaser P. 2021.

Evolution of VIM-1-producing *Klebsiella pneumoniae* isolates from a hospital outbreak reveals the genetic bases of the loss of the urease-positive identification character.

mSystems 6:e00244-21. <https://doi.org/10.1128/mSystems.00244-21>.

Editor Robert G. Beiko, Dalhousie University

Copyright © 2021 Cabanel et al. This is an open-access article distributed under the terms of the [Creative Commons Attribution 4.0 International license](https://creativecommons.org/licenses/by/4.0/).

Address correspondence to Philippe Glaser, pglaser@pasteur.fr.

Received 1 March 2021

Accepted 6 May 2021

Published 1 June 2021

KEYWORDS carbapenemase, insertion sequence, *Klebsiella pneumoniae*, drug resistance evolution, mobile genetic elements, urease

Klebsiella pneumoniae is responsible for a broad range of diseases including pneumonia and bloodstream and urinary tract infections, mostly in health care facilities. *K. pneumoniae* isolates are frequently resistant to multiple antibiotics and contribute to the dissemination of antibiotic resistance genes (ARGs) (1, 2). Carbapenems are among the last-resort drugs to treat infections due to multidrug-resistant (MDR) *Enterobacteriales*, including *K. pneumoniae* isolates expressing extended-spectrum β -lactamases (ESBLs). From the end of the 20th century onward, the emergence and dissemination of carbapenemase-producing *K. pneumoniae* (CPKp) resulting in high mortality rates have become a major public health threat. CPKp hospital outbreaks are particularly feared due to potential patient-to-patient transmission or transmission from the hospital environment to the patient. Recently, a broad genomic study on CPKp from 244 hospitals in 32 countries across Europe confirmed the existence of dominant lineages responsible for hospital outbreaks (3). In this study, the most prevalent multilocus sequence typing (MLST) types (STs) were from the clonal group (CG) 258, including ST258, -512, -340, -437, and -11, expressing the carbapenemase KPC (1, 3). Other prominent CPKp STs are ST307 (4) and ST101 (5). However, the molecular epidemiology of CPKp is different between countries (6), and a large proportion of CPKp isolates belongs to diverse and rare STs denoting relevance of local epidemiology.

In 2007, we reported the first case of a hospital outbreak involving CPKp isolates producing the VIM-1 carbapenemase in a hospital in Madrid, Spain (7, 8). During the same period, *Escherichia coli*, *Klebsiella oxytoca*, and *Enterobacter cloacae* isolates also producing VIM-1 were identified in the same hospital (7). Pulsed-field gel electrophoresis (PFGE) of *K. pneumoniae* isolates showed that they were likely clonal (8). This observation raised questions about the risk of endemicity of this clone and of the plasmid carrying *bla*_{VIM-1} (7).

Whole-genome sequencing (WGS) is becoming instrumental to decipher hospital outbreaks and to characterize transmission (9). Point mutations and small indels, particularly those leading to gene inactivation or contributing to antibiotic resistance, are the main focus of genomic epidemiology studies. Other events, and in particular the mobility of insertion sequences (ISs), more difficult to identify by short-read sequencing, are frequently set aside. In this work, we have analyzed the evolution of the VIM-1-producing *K. pneumoniae* isolates from the outbreak (7, 8). In addition to mutations selected by antibiotics used in the hospital, we observed a diversity in ARGs and plasmid contents and mobility of transposable elements: a group 2 intron and three ISs, IS26, IS5075, and IS421. In one isolate, IS5075 transposed into the *ure* operon encoding the urease subunits and led to a urease-defective phenotype. By analyzing 9,755 publicly available *K. pneumoniae* genome sequences, we show that this insertion is frequent, explaining why some *K. pneumoniae* isolates display a urease-negative phenotype. Furthermore, through a literature survey and the analysis of publicly available genome sequences, we did not find any evidence of further dissemination of this VIM-1-producing strain. On the other hand, the *bla*_{VIM-1} plasmid has broadly disseminated across *Enterobacteriales* species but so far has been isolated only in Spain.

RESULTS

Genomic characterization of the outbreak isolates. Illumina WGS of the 18 isolates and *in silico* MLST showed that the first 17 isolates (KP_{VIM1} to -17) sharing the same PFGE profile belong to ST39 and the last isolate (KP_{VIM18}) belongs to ST45 (see Table S1 in the supplemental material). ST45 represents 1.5% ($n = 161$) of the 10,515 genomes retrieved from NCBI (July 2020). ST39 is less frequent, with only 38 other genome sequences, including seven isolates carrying carbapenemase genes (*bla*_{KPC-3 γ} , $n = 3$; *bla*_{KPC-2 γ} , $n = 2$; *bla*_{NDM-1}, $n = 2$) but none carrying *bla*_{VIM-1}. In order to characterize the strain responsible for the outbreak and to identify genetic events occurring during its

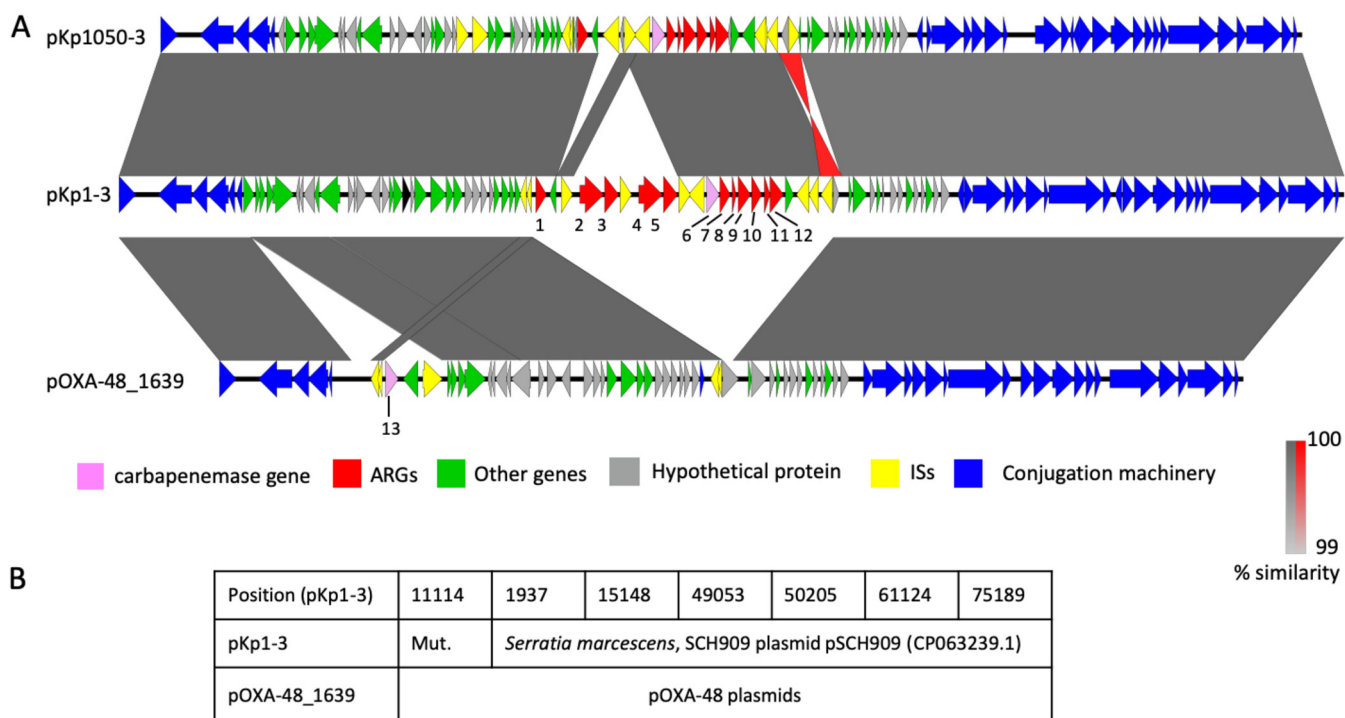


FIG 1 Comparison of pKp1-3, pKp1050-3, and pOXA-48. (A) Comparison of plasmids pKp1-3 and pKp1050-3 (accession no. CP023419.1) carrying *bla*_{VIM-1} and of pOXA-48_1639 carrying *bla*_{OXA-48} (accession no. LR025105.1). pOXA48_1639 was chosen as it was the closest relative to pKp1-3. Gray areas between open reading frames denote nucleotide identities with a gradient representing 99% (light gray) to 100% (dark gray) identity. Identities of an inverted region are represented in red. Genes are indicated by arrows with a color code as in the figure key. Antibiotic resistance genes are numbered as follows: 1, *catA1*; 2 and 4, *msrE_1*; 3 and 5, *mphE*; 6, *bla*_{VIM-1}; 7, *aacA4_2*; 8, *dfxB1*; 9, *ant1_2*; 10, *cat_2*; 11, *emrE*; 12, *folP_4*; 13, *bla*_{OXA-48}. (B) Analysis of the SNPs detected between pKp1-3 and pOXA-48_1639. Occurrences of SNPs among publicly available IncL/M plasmids were identified by BLASTN. SNP positions in pKp1-3 are indicated in the first line. Mut. indicates that the mutation is specific to IncL/M VIM-1 plasmids. For other positions, plasmids with the pKp1-3 allele or the pOXA-48_1639 allele are indicated in the second and third line, respectively. pSCH909 carries *bla*_{OXA-10} and *bla*_{TEM-1} but no carbapenemase gene.

evolution, we determined the complete genome sequence of the first isolate, KP_{VIM-1}. The KP_{VIM-1} chromosome is 5,351,626 bp long. It hosts four plasmids of 227,556 bp (pKP1-1), 110,924 bp (pKP1-2), 76,065 bp (pKP1-3), and 80,027 bp (pKP1-4) (Table S2). The chromosome and plasmids pKP1-1, -2, and -3 carry 31 ARGs, including three in two copies [*msr* (E), *mph*(E), and *sulI*] (Table S2). Those ARGs target all major classes of antibiotics used against Gram-negative bacteria. The porin gene *ompK35* is interrupted by a nonsense mutation at codon 230. In agreement with the ARG content, KP_{VIM-1} is highly resistant to almost all antibiotics tested, remaining susceptible to only ciprofloxacin, tigecycline, imipenem, and colistin and exhibiting an intermediate phenotype to amikacin, nalidixic acid, meropenem, and ertapenem (Fig. S1).

The *bla*_{VIM-1} gene is carried by a gene cassette inserted in a type 1 integron expressing six ARGs in addition to *bla*_{VIM-1} (*aacA4*, *dfxB1*, *ant1*, *cat*, *emrE*, and *folP_4*) carried by plasmid pKp1-3 (Fig. 1). BLASTN search using the nucleotide sequence of this plasmid against the contigs of KP_{VIM-18} showed 100% identity over its entire length, except a 1,722-bp region containing a *catA* gene and missing in KP_{VIM-18}. The VIM-1 plasmid was therefore likely transferred in the hospital from the outbreak strain to the ST45 *K. pneumoniae* isolate. Plasmid pKp1-3 belongs to the IncL/M type. Comparison with complete plasmid sequences showed that pKp1-3 is more than 99.9% identical over 89% of its length to pKp1050-3b carrying *bla*_{VIM-1} from a pan-drug-resistant *K. pneumoniae* strain isolated in June 2016 in a hospital in Madrid (Fig. 1) (10). Both plasmids are highly similar to a *bla*_{VIM-1}-carrying plasmid from a *Salmonella enterica* serovar Typhimurium strain isolated in Spain in 2014 (11) and from *Klebsiella oxytoca* strains isolated in Madrid in 2016 (12). Recently, a closely related plasmid was identified in 28 *Serratia marcescens* VIM-1-producing isolates recovered in our hospital as KP_{VIM-1} between September 2016 and December 2018 (13). We identified by BLASTN search 10 additional *K. pneumoniae*

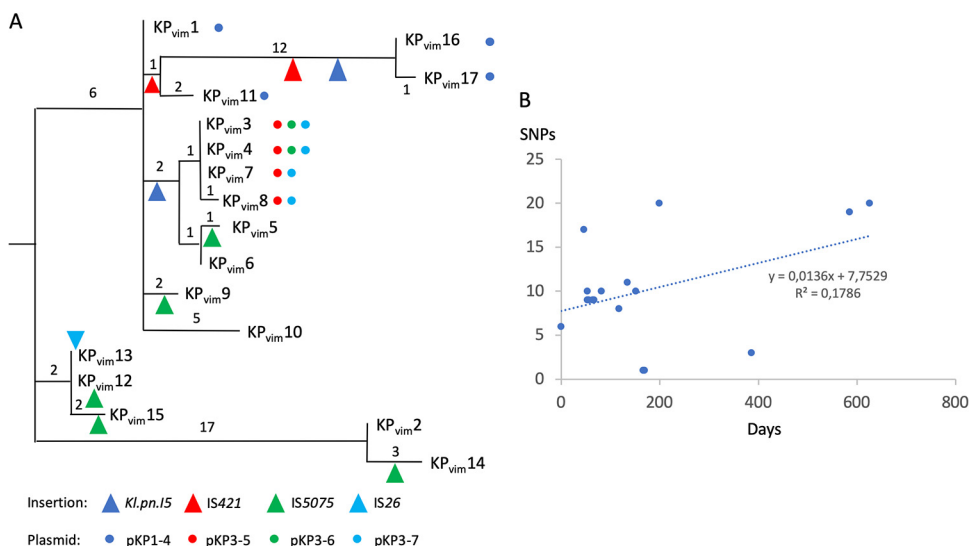


FIG 2 Hospital evolution of the *K. pneumoniae* ST39 VIM-1-producing strain. (A) Phylogeny of the 17 isolates reconstructed by maximum parsimony. Numbers next to branches indicate the number of chromosomal SNPs in the corresponding branch. Presence of plasmids is indicated by colored points, and transposition events are indicated by triangles. IS26 insertion in *oqxR* occurred in the common ancestor of KP_{VIM}12 and KP_{VIM}13. (B) Root-to-tip representation of the number of chromosomal SNPs according to the time (in days) following the isolation of the first isolate, KP_{VIM}1. The trendline equation and the correlation coefficient are indicated on the graph.

isolates carrying a plasmid closely related to pKP1-3, among the 85 *K. pneumoniae* genome sequences containing *bla*_{VIM-1} of the 10,515 *K. pneumoniae* genome sequences from the NCBI (Table S3). Strikingly, these isolates from four different STs were also all isolated in Spain between 2010 and 2016. Therefore, IncL/M plasmids carrying *bla*_{VIM-1} likely arose in Spain following the insertion of a type 2 integron and disseminated locally only but were recurrently isolated in Spain between 2005 and 2018.

These plasmids are closely related to the broadly distributed IncL/M plasmid pOXA48 carrying the *bla*_{OXA-48} carbapenemase gene (10) (Fig. 1). pKP1-3 shows only seven single nucleotide polymorphisms (SNPs) over 57,386 conserved bp with pOXA-48_1639, the closest relative identified at the NCBI (accession number [LR025105.1](https://www.ncbi.nlm.nih.gov/nuccore/LR025105.1)). BLASTN search against the NCBI database showed that one SNP was specific to all characterized IncL/M VIM-1 plasmids, whereas for the six other positions, two different allelic forms could be identified: one shared by pOXA-48_1639 and other pOXA-48 plasmids, the other by pKP1-3 and IncL/M plasmids carrying other resistance genes. Therefore, these two plasmids share a very recent common ancestor which acquired either Tn1999 (14) carrying *bla*_{OXA-48} or an integron carrying *bla*_{VIM-1}.

Intrahospital evolution of the ST39 lineage follows different paths associated with modifications of antibiotic susceptibility. On the basis of the variants identified, we reconstructed the evolutionary path of the 17 ST39 isolates (Fig. 2A). In total, we identified 64 SNPs (59 in the chromosome and five in the plasmids) and seven short indels, five of them leading to a frameshift in coding frames (Table S4). Ancestral genotype for each polymorphism was predicted by parsimony based on BLASTN comparisons with complete *K. pneumoniae* genome sequences at the NCBI. The first isolate, KP_{VIM}1, shows six SNPs compared to the reconstructed sequence of the last common ancestor (LCA) of the 17 isolates. We next analyzed the root to tip number of chromosomal SNPs according to the time of isolation. Despite the duration of the outbreak over 24 months, we did not observe a strong temporal correlation (Fig. 2B).

We identified three large chromosomal deletions: a 6.3-kb deletion encompassing *mgrB*, a 600-bp deletion of a type 6 secretion system (T6SS) immunity phospholipase A1-binding lipoprotein, and a 55.4-kb deletion corresponding to the excision of an integrated and conjugative element. Five large deletions in pKP1-1 and pKP1-2 led to

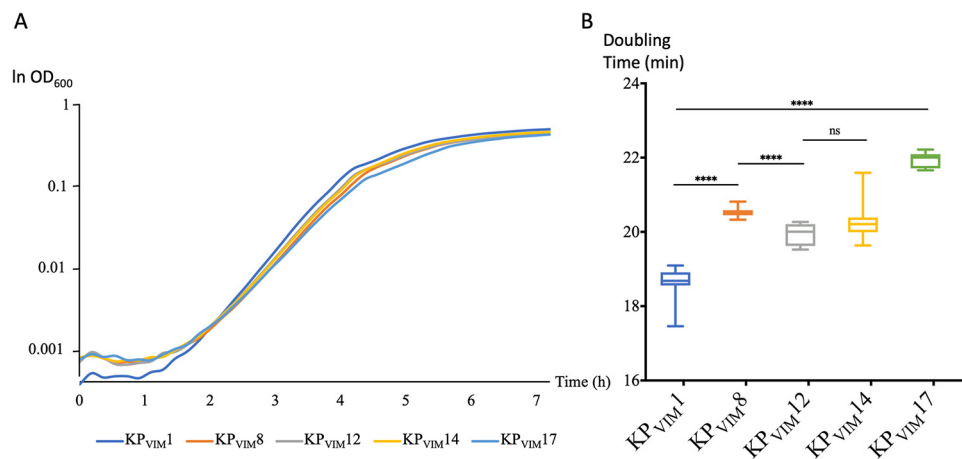


FIG 3 Growth and generation times of isolates with decreased antibiotic susceptibility. (A) Growth of KP_{VIM1} and of four isolates mutated in a repressor of efflux pumps (KP_{VIM8}, KP_{VIM12}, and KP_{VIM14}) or in *mgrB* and *ompK36* (KP_{VIM17}) was followed by using an automatic plate reader. Background was subtracted as described in Materials and Methods. During the first 90 min, the OD₆₀₀ was below 0.0015, and its quantification is noisy. (B) Box plot representation for 10 replicates of the generation times of the five isolates quantified in early exponential phase 2.5 h following the start of the culture (OD₆₀₀ between 0.005 and 0.04). Statistical significances were tested with Student's *t* test. ****, $P \leq 0.0001$; ns, nonsignificant.

the loss of clusters of ARGs (Table S2 and S4) in agreement with modifications of the antibiotic susceptibility profiles (Fig. S1).

Several genetic events were likely selected in response to antibiotic use in the hospital. The deletion of the *mgrB* gene led to colistin resistance in KP_{VIM17} (Fig. S1). The same isolate was highly resistant to all β -lactams including carbapenems due to the inactivation of the second major porin gene, *ompK36*, by a nonsense mutation leading to a stop codon at position 125. In addition, we identified three mutations disrupting *oqxR* and *ramR* genes encoding repressors of efflux systems. *oqxR* was inactivated by an IS26 insertion in KP_{VIM12} and KP_{VIM13}, whereas *ramR* was inactivated by a nonsense mutation in KP_{VIM14} and by a frameshift mutation in KP_{VIM7} and KP_{VIM8}. In agreement with previous comparisons of mutants of *oqxR* and *ramR* (15–18), we observed a stronger decrease in the susceptibility to fluoroquinolones in the isolates mutated in *oqxR* (KP_{VIM12} and KP_{VIM13}) and a stronger decrease in tigecycline susceptibility in the isolates mutated in *ramR* (KP_{VIM7}, -8, and -14). In the case of KP_{VIM14}, the mutation in *ramR* likely compensates the loss of the *qnrA1* gene for fluoroquinolone susceptibility. The five isolates also showed a decreased susceptibility to cefepime and ceftazidime (Fig. S1). To assess if there was any fitness cost associated with the increased resistance observed, we followed bacterial growth of these isolates in LB at 37°C. We observed in all four mutated isolates a decreased growth rate compared to KP_{VIM1}. The effect was more pronounced for KP_{VIM17} defective in both *mgrB* and *ompK36*, which showed a 17% increase of generation time (Fig. 3).

Diversity of cryptic plasmid content. In the course of the epidemic strain evolution, we also observed changes in plasmid content (Fig. 2). Plasmid pKP1-4 is a IncFII type, which is present in the first isolate, KP_{VIM1}, and in three of the last isolates of the outbreak (KP_{VIM11}, -16, and -17), reflecting its stability. This plasmid mainly codes for maintenance functions (toxin-antitoxin systems, colicin B production, and partition) and conjugative functions. BLASTN search against bacterial genome sequences showed that pKP1-4 is almost identical (99.7% identities over its entire length) to plasmid pEC14III (accession number [KU932028.1](https://pubmed.ncbi.nlm.nih.gov/31111111/)) from an *E. coli* strain isolated in Finland. We also identified three plasmids specific to the lineage KP_{VIM3} to KP_{VIM8} (Fig. 2). These six isolates share a 34,017-bp-long, linear plasmid (pKP3-5) flanked by two 695-bp-long terminal inverted repeats (TIRs). Unlike most linear plasmids described in *K. pneumoniae*, pKP3-5 is unrelated to phages. No adaptive functions were recognized, unlike in a

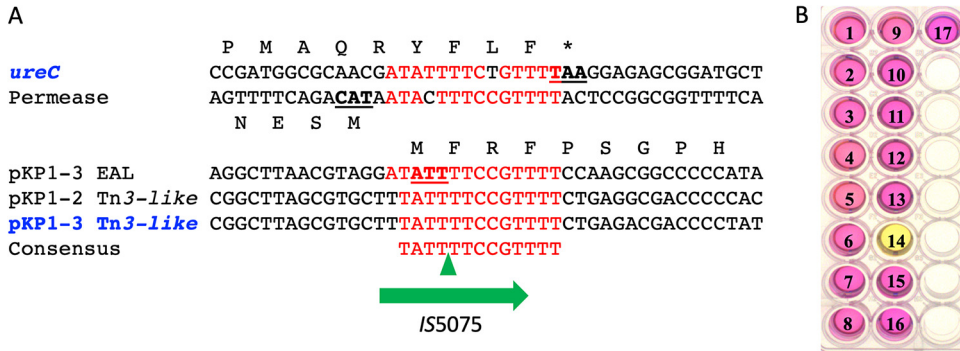


FIG 4 Urease inactivation following IS5075 transposition. (A) Sequence alignment of the sites targeted by IS5075 among KP_{VIM} isolates. In blue, targets of transposition events occurring during the outbreak: *ureC* in KP_{VIM}14 and pKP1-3 Tn27 in KP_{VIM}5, KP_{VIM}9, KP_{VIM}12, and KP_{VIM}15. The green triangles correspond to IS5075 insertion sites. Conserved bases are indicated in red. Stop and start codons are underlined. (B) Urease activity test of the 17 ST39 isolates. The number of each KP_{VIM} isolate is indicated on the well. A pink color of the indole reaction reveals a urease-positive phenotype.

similar linear plasmid, pBSSB1 from *Salmonella enterica* serovar Typhi, that encodes a flagellin structural gene (19). A search among *K. pneumoniae* genomes revealed 19 isolates carrying putative linear plasmids closely similar to pKP3-5 (>90% identities over 90% of the length). The two other plasmids are small high-copy-number plasmids, pKP3-6 (2,811 bp) and pKP3-7 (3,861 bp), that are present in strains KP_{VIM}3 to -6 and KP_{VIM}3 to -8, respectively (Fig. 2 and Table S2). No adaptive functions were predicted in these two plasmids. For these three plasmids, we could not determine whether they were gained in the common ancestor of the KP_{VIM}3 to KP_{VIM}8 clade or lost by other isolates.

Insertion of IS5075 into *ureC* is responsible for a urease-negative phenotype in one isolate of the outbreak. In addition to IS26 insertion in *oqxR*, we identified nine transpositions of mobile genetic elements: two insertions of a class 2 intron named *Kl.pn.15* (20) and two and five transpositions of IS421 and IS5075, respectively (Fig. 2). Compared to the other isolates, KP_{VIM}14 was characterized by an IS5075 inserted three codons upstream of the stop codon of the *ureC* gene encoding the urease catalytic subunit (Fig. 4A). This insertion led to a *ureC*-IS5075 transposase gene fusion. It might also have a polar effect on the expression of the downstream genes of the operon: *ureE*, *ureF*, and *ureG*. Accordingly, the KP_{VIM}14 isolate was urease negative, whereas all other isolates from the outbreak were urease positive (Fig. 4B). IS5075, like its close relative IS4321, is known to transpose into the TIR of Tn21 and of related transposons of the Tn3 family (21). Tn3 family transposons are abundant and diverse (22). They are vectors of heavy metal resistance and ARGs (21). The 17 ST39 isolates harbor three copies of IS5075 inserted in a pKP1-2 Tn3 family transposon, just after the initiation codon of a pKP1-1 gene coding for an EAL motif protein and upstream of a chromosomal permease gene (Fig. 4A). Four independent and identical transposition events of IS5075 also occurred in the TIR of a Tn3 family transposon carried by pKP1-3, in KP_{VIM}5, KP_{VIM}9, KP_{VIM}12, and KP_{VIM}15 (Fig. 2A). Based on the conservation of the insertion sites of IS5075, we proposed a 13-bp consensus sequence for the IS5075 transposition site (Fig. 4A).

Urease-negative phenotypes are prevailing in several *K. pneumoniae* MDR lineages. Urea hydrolysis is an identification trait of *K. pneumoniae* in clinical microbiology laboratories. However, earlier reports have shown that 5% of *K. pneumoniae* isolates are urease negative (23). In order to determine whether this phenotype was due to similar IS5075 transposition, we analyzed the *ureC* gene in 9,755 *K. pneumoniae* genomes quality filtered from the 10,515 genome sequences retrieved from the NCBI (Table S5). BLASTN search showed that an IS5075 or a similar IS was inserted at the same position in 1,380 isolates (14.1%) (Table 1). A search for other insertions or

TABLE 1 Comparison of *ureC*::IS5075 and *ureC* WT *K. pneumoniae* isolates for antibiotic resistance features and ARG and IS copy numbers

		All	<i>ureC</i> WT	<i>ureC</i> ::IS5075	<i>P</i> value ^e
No. of isolates ^a	All isolates	9,755 ^a	8,375	1,380 (14.1% ^b)	
	Minus ST11 and ST14	7,978	7,540	438 (5.4% ^b)	
<i>gyrA</i> or <i>parC</i> QRDR mutated	All isolates	6,062	4,763 (55.9% ^c)	1,299 (94% ^d)	1e−153
	Minus ST11 and ST14	4,367	4,009 (53.2% ^c)	358 (81.7% ^d)	3e−31
Carbapenemase gene	All isolates	5,146	3,953 (47.2% ^c)	1,193 (86.4% ^d)	6.3e−161
	Minus ST11 and ST14	3,677	3,393 (45% ^c)	284 (64.8% ^d)	8.4e−16
Carbapenemase gene and <i>gyrA</i> or <i>parC</i> mutated	All isolates	4,549	3,376 (40.3% ^c)	1,173 (85% ^d)	2.2e−208
	Minus ST11 and ST14	3,093	2,829 (36.5% ^c)	264 (60.2% ^d)	3.3e−21
Avg no. of IS5075 and related ISs	All isolates	1.82	1.31	5	0
	Minus ST11 and ST14	1.45	1.27	5.11	4.2e−207
Avg no. of ARGs	All isolates	9.33	8.81	12.5	4.3e−101
	Minus ST11 and ST14	8.7	8.51	11.74	1.6e−23

^aAfter filtering out 760 genome sequences out of the 10,515 sequences retrieved from the NCBI.

^bPercentage of isolates with an IS insertion in *ureC*.

^cPercentage of *ureC* WT isolates mutated in QRDR and/or carrier of carbapenemase genes.

^dPercentage of *ureC*::IS5075 isolates mutated in QRDR and/or carrier of carbapenemase genes.

^eSignificance of the difference between *ureC*::IS5075 and *ureC* as determined by the chi-square or the Wilcoxon rank sum statistical test.

frameshifts in *ureC* did not reveal other frequent mutations putatively responsible for a urease deficiency.

To determine whether the insertion of IS5075 into *ureC* preferentially occurred under specific genetic backgrounds, we analyzed the 45 *K. pneumoniae* STs with at least 20 isolates (Fig. 5). We observed that IS5075 urease inactivation occurred throughout the species with variable frequencies. In seven STs, all with fewer than 100 isolates, no insertion was observed. On the other hand, we observed a high proportion of *ureC*::IS5075 isolates in some STs like ST11 (884 out of 1,603) and ST340 (18 out of 77 isolates) from the clonal group (CG) 258 and ST14 (58 out of 174). On the other hand, the two other dominant CG258 STs, ST258 and ST512, showed lower insertion frequencies of 6.9% and 4.1%, respectively.

As several of the STs associated with a higher frequency of *ureC*::IS5075 include major MDR lineages, we next analyzed the distribution of IS insertions in *ureC* in relation to antibiotic resistance. As markers of antibiotic resistance, we considered mutations in fluoroquinolone resistance (FQR) determinants, presence of carbapenemase genes, and the number of ARGs among the 9,755 *K. pneumoniae* genome sequences (Table S5). Among these genome sequences, 62% were mutated in *gyrA* and/or *parC* quinolone resistance-determining regions (QRDRs), 53% carried carbapenemase genes, and the average number of ARGs was 9.33, revealing a strong bias toward MDR isolates (Table 1). Despite this bias, *ureC*::IS5075 isolates appeared as even more resistant, with an average number of 12.5 ARGs compared to 8.8 in the remaining isolates, 94% of the isolates showing mutations in *gyrA* and/or *parC* and 86.4% carrying a carbapenemase gene (Table 1). To determine whether the insertion in *ureC* was associated with a global expansion of IS5075 and related ISs, we estimated the copy number of these ISs in the different isolates (Table 1). Isolates with an IS insertion in *ureC* showed on average a 4-fold-higher copy number of IS5075 and related ISs than the remaining isolates (5 versus 1.31). On the other hand, more than half of the isolates with an intact *ureC* gene did not carry a single IS5075 copy (4,334 out of 8,375).

In a given ST, a high frequency of *ureC*::IS5075 isolates might result from frequent transposition events or from the expansion of lineages carrying the insertion. To discriminate between these two possibilities, we performed a whole-genome phylogeny focusing on ST11, ST14, and ST258. ST11 was the most abundant ST among the genome sequences retrieved from the NCBI (16.4% of all isolates). Except two isolates

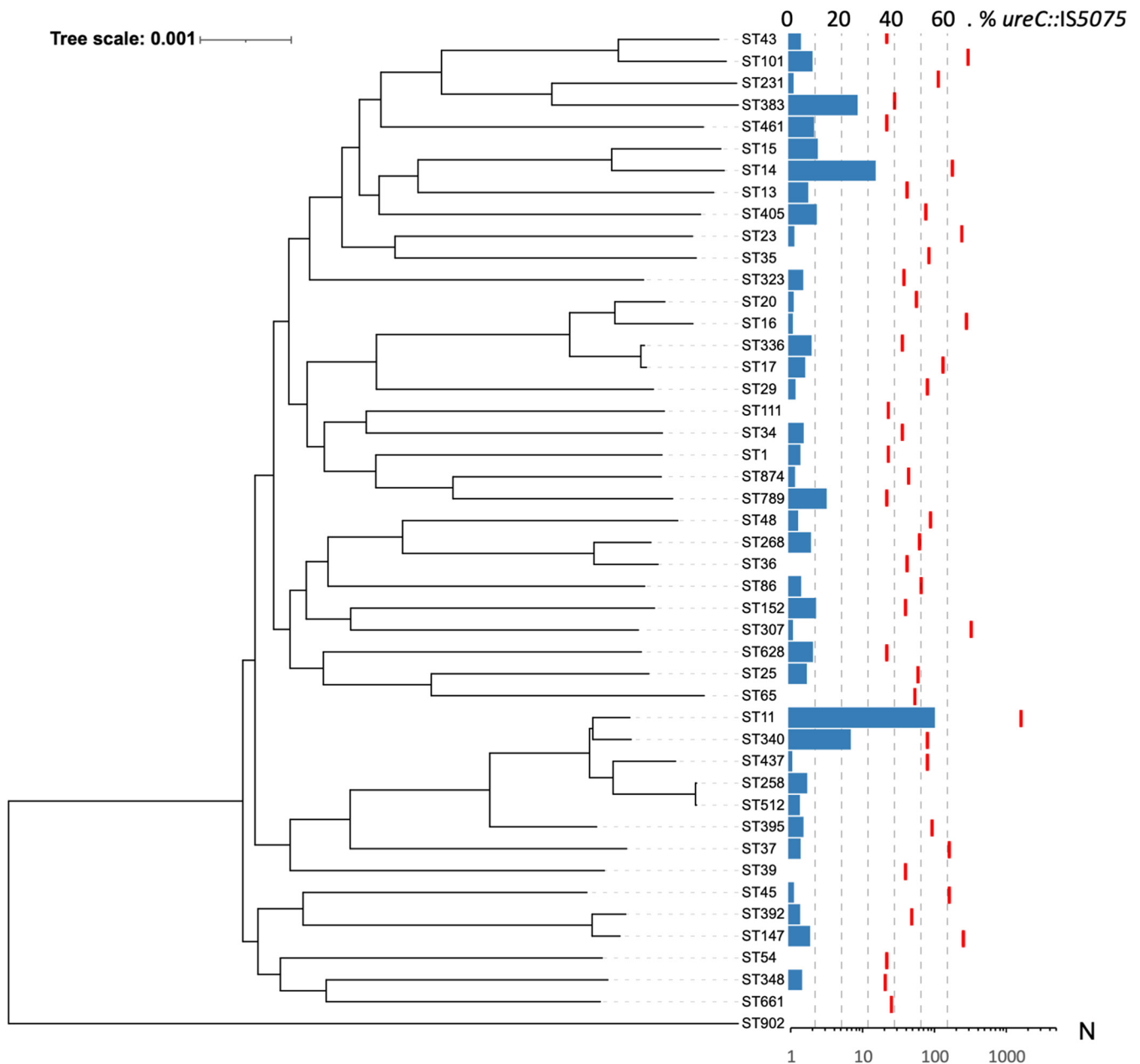


FIG 5 Distribution of IS5075 insertions in *ureC* among *K. pneumoniae* isolates. Occurrence of IS5075 insertion among the 45 STs with at least 20 isolates among 9,755 *K. pneumoniae* genome sequences retrieved from the NCBI. Phylogeny was reconstructed using Parsnp (50) and by using a representative isolate from each ST. The tree was rooted according to the work of David et al. (3). Blue bars indicate the percentage of isolates with an insertion in *ureC* (upper scale), and red dashes indicate the number of isolates in the corresponding ST (lower scale).

that were wild type (WT) for *gyrA* and *parC*, all ST11 isolates were predicted to be FQR (Fig. 6). The two most populated lineages belong to the K-types KL64 ($n = 622$) and KL47 ($n = 463$). These closely related lineages share the same three mutations in QRDRs (ParC-80I, GyrA-83I, GyrA-87G) and carry the carbapenemase gene *bla*_{KPC-2}. Analysis of IS5075 insertions in *ureC* showed an uneven distribution, mostly associated with these two lineages. In the KL64 clade, the IS insertion is ancestral, as it was present in all except six isolates (in pink). In the KL47 clade, two different situations were noted: an ancestral transposition event in the LCA of a specific sublineage, with the 138 isolates from this clade showing an IS5075 in *ureC* (clade colored in red), and a relatively high frequency of insertion in the other isolates of the clade (85 out of 324, 26%) likely

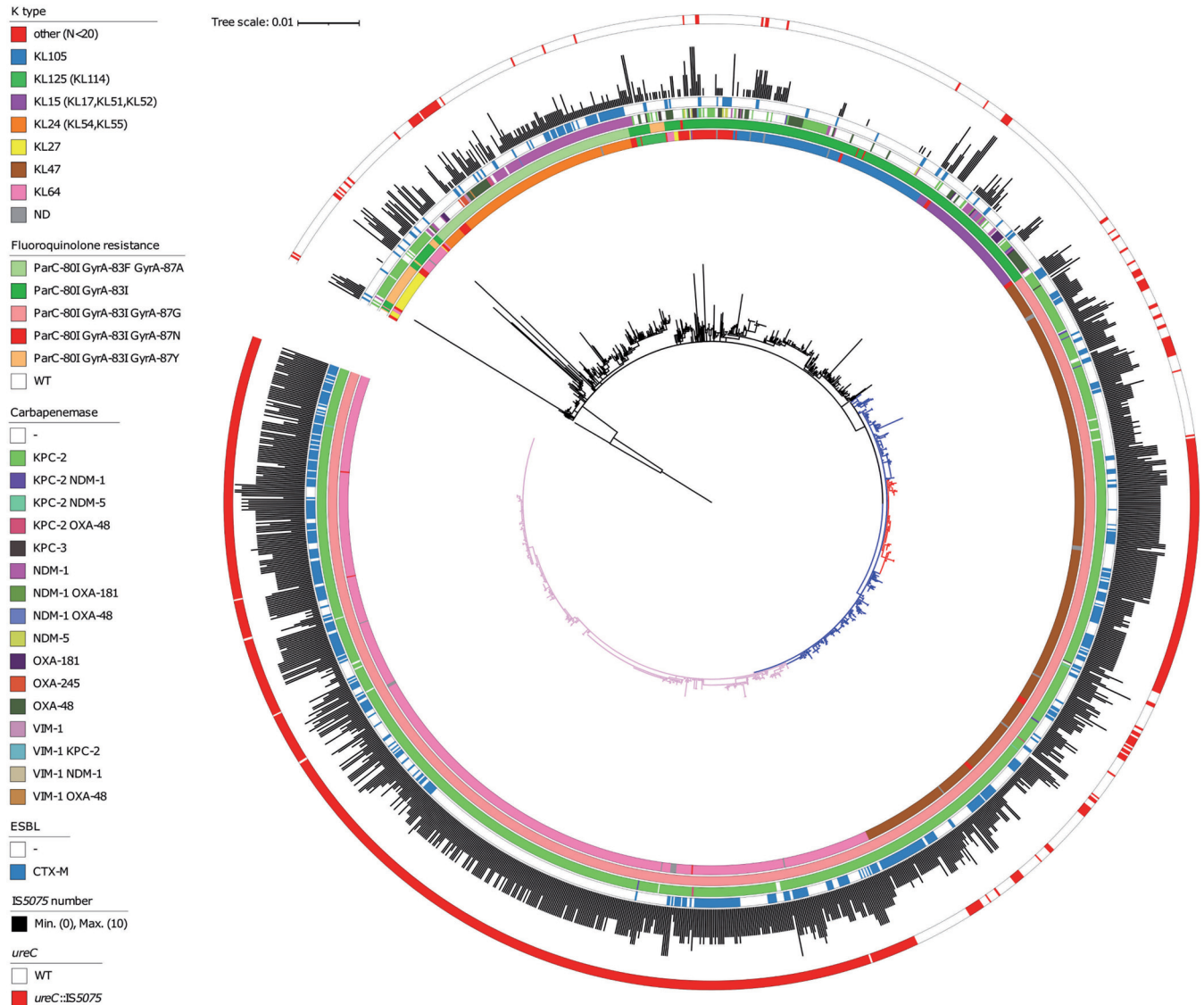


FIG 6 Core genome phylogeny of *K. pneumoniae* ST11 isolates. Phylogeny was obtained by using Parsnp (50) considering 1,603 genomes passing the quality threshold. K-type, mutations in *gyrA* and *parC* QRDRs, carbapenemase genes, *bla*_{CTX-M} genes, copy number of IS5075 and related ISs, and IS insertion in *ureC* are annotated by circles from inside to outside as indicated in the figure key (left). The *ureC*-deficient KL64 lineage is in pink. The KL47 lineage is in blue, and the *ureC*-deficient sublineage is in red. The two *gyrA/parC* WT isolates were used as outgroups to root the tree. The tree was visualized by using iTOL (51). ND, no data.

resulting from multiple sporadic transposition events. Out of the two clades, the frequency of insertion is much lower (8.5%). All over the ST11 phylogeny, insertion in the *ureC* gene was associated with a higher copy number of IS5075 with on average 5 copies compared to 1.7 in ST11 isolates with a WT *ureC* gene. Altogether, these results show that the high proportion of ST11 isolates mutated in *ureC* results in a large part from the dissemination of two clades showing a high number of IS5075 copies. The situation was similar among ST14 isolates, as all but one isolate ($n = 58$) mutated in *ureC* belonged to a single FQR lineage, suggesting that transposition occurred in the LCA of the lineage (in blue, Fig. S2). Isolates of this lineage also showed a high IS5075 copy number ($n = 5.1$). In ST258, isolates were characterized by a lower frequency of IS insertion in *ureC* (6.9%). Most of the ST258 isolates cluster in two lineages expressing two different capsule operons of K-types KL106 and KL107 and associated mostly with the carbapenemase genes *bla*_{KPC-2} and *bla*_{KPC-3}, respectively (24). In contrast to what was observed in ST11 and ST14, no expansion of a large *ureC*::IS5075 clade occurred

(Fig. S3). All but two isolates with the insertion in *ureC* belonged to the KL107 lineage. Strikingly, this clade was characterized by a higher copy number of *IS5075* of 2.17 (5.24 for *ureC::IS5075* isolates) compared to only 0.12 for the KL106 lineage. Therefore, a major driver for insertion into *ureC* is the presence of an *IS5075* or a related IS and its active transposition.

DISCUSSION

Whole-genome sequencing has revolutionized molecular epidemiology, and its use in outbreak analysis has contributed to deciphering the path of pathogen transmission (25). Here, we investigated the first outbreak due to a VIM-1-producing *K. pneumoniae* strain in Spain (7, 8). The strain was extensively drug resistant and belongs to an uncommon ST (ST39). Based on available genomic data, we showed that the strain pre-existed in the hospital prior to the identification of the first isolate in October 2005. Furthermore, the weak temporal signal in the evolution (Fig. 2B) indicated a likely environmental reservoir in the hospital, which agrees with epidemiological data (7). Molecular clocks for *K. pneumoniae* evolution have been estimated between 1.4 (26), 1.9 (27), and 3.65 (28) mutations/ 10^6 bp/year. Here, the rate of SNPs/ 10^6 bp/year is in the lower range ($n=0.87$). Growth as a biofilm compared to planktonic growth has been related to a greater diversity due to its structured organization but a lower mutation rate due to a reduced number of generations (29). The diversity observed, the duration of the outbreak, and the small number of SNPs agree with a biofilm source of the isolates. In line with this observation, we observed biofilm production of all the isolates but to variable levels (see Fig. S4 in the supplemental material).

During the 2-year evolution of the strain, we observed variations in the antibiotic resistance profile. This was due on the one hand to the loss of ARGs (Table S4). On the other hand, mutations leading to the increased expression of efflux pumps or to a decreased drug permeation, and subsequently to a decreased susceptibility to some antibiotics, were selected. However, these mutations led to a fitness cost (Fig. 3), which might explain their limited expansion in the hospital.

By combining genomic analysis of the strain responsible for the outbreak with global genomic information retrieved from the NCBI and data from the literature, we were able to draw more general conclusions related to the risk associated with the outbreak strain and the VIM-1 plasmid. Likewise, we were able to identify the main reason for urease deficiency among *K. pneumoniae* isolates. Following the identification of the first VIM-1 isolates in Spain, their dissemination was a matter of concern (7). Although we showed that one single ST39 clone, except for one isolate, was responsible for the outbreak, we did not identify any new occurrence of this strain or of an ST39 isolate carrying *bla*_{VIM-1} based on bibliographical survey and on the analysis of more than 10,000 publicly available *K. pneumoniae* genome sequences. Therefore, this clone seems to be restricted to the hospital where it was isolated. Conversely, we showed that the plasmid carrying *bla*_{VIM-1} has disseminated among various Enterobacteriales species. Transfers occurred probably in the hospital context, as suggested in the case of an *S. Typhimurium* isolate (11). Similarly, we showed the transmission of the VIM-1 plasmid between *K. pneumoniae* isolates in the course of the outbreak. We previously predicted similar transfers between *K. pneumoniae* and *E. coli* based on plasmid typing and size determination (7). This IncL/M plasmid is closely related to the broadly disseminated pOXA48. Our mutation analysis strongly suggests independent gain of a carbapenemase gene by very similar plasmid backbones showing only seven SNPs over 57,386 bp. In agreement with this hypothesis, the first OXA-48 plasmid was detected in Spain in 2009 (30), 4 years after the first VIM-1 isolate of the hospital outbreak (7).

Strikingly, until now only IncL/M VIM-1 plasmids were reported in Spain. A recent study on plasmids encoding VIM-1 from broad origins showed that among the 28 plasmids analyzed, nine were from IncL/M type (31). These nine plasmids were related to pKP1-3 and were from *K. pneumoniae*, *Enterobacter hormaechei*, and *E. cloacae* and all from Spain. The limited dissemination of the VIM-1 plasmid might be due to the

conjunction of different factors including: a lower conjugation efficiency than pOXA-48 plasmids, a fitness cost restricting its dissemination to environments characterized by strong selective pressures, such as the hospital, or a specificity in antibiotic prescription in Spain. Comparing InCL/M VIM-1 and OXA-48 plasmids provides a model system to study two closely related plasmids with two different spreading destinies.

Urease is considered in many bacterial species as a virulence factor beyond its contribution in harnessing urea as a nitrogen source (32). Urease participates in the adaptation to acidic conditions in a broad range of human pathogens, including *Helicobacter pylori* (33), *Yersinia enterocolitica* (34), and *Proteus mirabilis* (35). Urease is considered a potential target for the development of new antibacterial drugs against enteric bacteria including *K. pneumoniae* (36). In *K. pneumoniae*, the urease has been shown to contribute to gastrointestinal colonization (37). However, a significant proportion of *K. pneumoniae* isolates are urease negative. Here, we showed that the inactivation of the operon is due to the transposition into the *ureC* gene of IS5075 or of related ISs, like IS4321, sharing the same specificity. Urease inactivation can be observed in both carriage isolates and isolates associated with clinical symptoms. For instance, we identified a cluster of eight IS5075::*ureC* ST340 isolates from a single institution (Fig. S5). These isolates were recovered from three patients, from urinary tract infections, blood culture, cerebrospinal fluid, and fecal carriage (38).

Among *ureC*::IS5075 isolates, we observed a higher prevalence of *gyrA* and *parC* mutations and of carbapenemase genes and, more generally, a higher number of ARGs compared to *ureC* WT isolates (Table 1). This was partly due to a small number of MDR lineages mutated in *ureC*, such as those of ST11 and ST14, which represent 68% of the *ureC*::IS5075 isolates (Fig. 6 and Fig. S2). Nevertheless, this higher prevalence remained true even after removing ST11 and ST14 isolates (Table 1). IS insertions in *ureC* were also associated with a 4-fold increase in IS5075 copies, resulting from additional transposition events (Table 1). This expansion of IS5075 in some genetic backgrounds might be a relatively recent event. Indeed, 44% of the isolates did not carry a single IS5075 copy, despite the high number of ARGs in the genomes we have analyzed. Indeed, the most frequent targets of IS5075 are the conserved TIR of transposons related to Tn21, which are ARG vectors and frequently carried by conjugative plasmids as in the case of pKP1-2 (21, 22). This insertion specificity represents a safe harbor for these ISs, as it does not incur fitness costs and ensures their dissemination. The insertion into *ureC* results from the high similarity between its last codons and TIRs of Tn21 and is likely accidental. Therefore, the higher frequency of *ureC* inactivation in some MDR lineages might merely be a consequence of a more frequent acquisition of Tn3 family transposons carrying IS5075. However, we cannot completely dismiss the possibility that the loss of urease activity might provide MDR *K. pneumoniae* isolates with a selective advantage under some circumstances. This seems rather unlikely, as other *ureC* inactivation events, including transpositions of other ISs, would have been expected in that case and we did not detect such events. Overall, IS5075 transposition into the *K. pneumoniae ureC* gene represents a perfect example of chromosomal colonization by IS elements carried by plasmids and leading to a homoplasic loss of function.

MATERIALS AND METHODS

Bacterial strains, growth conditions, and antibiotic susceptibility testing. VIM-1-producing *K. pneumoniae* isolates were collected from 2005 through 2008 at Ramon y Cajal University Hospital in Madrid, Spain (8) (see Table S1 in the supplemental material). The colistin MIC was determined in Mueller-Hinton (MH) broth as recommended by the Clinical and Laboratory Standards Institute (CLSI) guidelines (39). Susceptibility to 33 other antibiotics (Fig. S1) was evaluated by disk diffusion on MH agar according to the CLSI guidelines (39). Fitness was determined by growth curve analysis with a Tecan Infinite M200 automatic spectrophotometer during 24 h in LB. Wells were inoculated with overnight cultures at an optical density at 600 nm (OD₆₀₀) of 0.001. OD₆₀₀ was measured every 10 min. Background was determined as the average value of the OD₆₀₀ of the first three time points. Doubling time was determined between OD₆₀₀s of 0.005 and 0.03, where an almost perfect fit with an exponential growth was observed.

Genome sequencing and sequence analysis. *K. pneumoniae* genomes were sequenced by using the Illumina HiSeq2500 platform, with 100-nucleotide (nt) paired-end reads. Libraries were constructed by using the Nextera XT kit (Illumina). Reads were assembled with SPAdes 3.9.0 (40). The complete genome sequence of strain KP_{VIM}1 was determined by using the long-read PacBio technology (Macrogen, Seoul, South Korea). Reads were assembled with the RS_HGAP_Assembly.3 protocol (41) and with Canu (42). The consensus sequence was polished with Quiver (41) and manually corrected by mapping Illumina reads with Breseq 0.33.2 (43). Variants compared to KP_{VIM}1 were identified by using Breseq (43). Genome sequences were annotated with Prokka 1.14.5 (44) and analyzed for MLST and ARG content by using Kleborate (45) and Resfinder 4.0.1 (46). Plasmid incompatibility groups were identified by using PlasmidFinder 2.1 (47). Directionality of mutations was determined as previously described by performing BLASTN comparisons against publicly available *K. pneumoniae* genomes (48).

Analysis of publicly available genome sequences. *K. pneumoniae* genome assemblies ($n = 10,515$) were downloaded from the NCBI (July 2020) with Batch Entrez (49). Genome sequences with more than 200 contigs of more than 500 nt were filtered out. Sixty genome sequences (BioProject [PRJNA510003](#)) for which the contig ends corresponding to repeated sequences have been trimmed were removed from the analysis. In total, we analyzed IS5075 insertions in 9,755 genome sequences (Table S5). Phylogenetic analysis was performed by using Parsnp 1.1.2 (50). Recombination regions were visually identified as regions with a higher SNP density by using Gingr (50) and removed from the reference genome sequence (ST11, strain FDAARGOS_444, [CP023941.1](#); ST14, strain 11, [CP016923.1](#); ST258, strain BIC-1, [NZ_CP022573.1](#); ST340, strain EuSCAPE_RS081, GCA_902155965.1_18858_1_51). Insertion of IS5075 and of related ISs in *ureC* was identified by BLASTN search using as query sequence the junction sequence detected in the KP_{VIM}14 isolate encompassing 20 nt of the *ureC* gene and 20 nt of IS5075 (E value of $1e-10$ as threshold). The integrity of *ureC* was tested by tBLASTn using the UreC protein sequence from KP_{VIM}1 as query. Copy number of IS5075 and of closely related ISs was estimated by counting BLASTN hits (100% identity over the entire length), using the first 17 nucleotides of the IS5075 sequence as query. Phylogenetic trees were visualized by using iTOL (51).

Phenotypic analyses. The urease detection test was carried out with urea-indole medium (Bio-Rad) according to the manufacturer's instructions. Biofilm formation capacity was measured by the microtiter plate assay as previously described (52). *K. pneumoniae* strain LM21 (53) was used as a positive control.

Statistical analysis. The significance of the differences in frequencies of IS insertions in *ureC* was determined by using the chi-square test. The significance of differences in IS5075 copy numbers and in ARG numbers was determined by the Wilcoxon rank sum test. Both tests were performed by using standard libraries contained within the R statistics package (<http://www.R-project.org/>). Statistical significances of growth rate differences were tested with a Student *t* test.

Availability of data. All sequence data have been deposited at DDBJ/EMBL/GenBank (BioProject [PRJEB41835](#)) with the following accession numbers: [LR991401](#), KP_{VIM}1 chromosome and plasmids; [LR991487](#), plasmid pKP1-5; [LR991544](#), plasmid pKP1-6; [LR991565](#), plasmid pKP1-7. BioSample identifiers for the Illumina sequence data are listed in Table S1.

SUPPLEMENTAL MATERIAL

Supplemental material is available online only.

FIG S1, PDF file, 0.1 MB.

FIG S2, PDF file, 0.2 MB.

FIG S3, PDF file, 0.7 MB.

FIG S4, PDF file, 0.1 MB.

FIG S5, PDF file, 0.1 MB.

TABLE S1, PDF file, 0.03 MB.

TABLE S2, PDF file, 0.03 MB.

TABLE S3, PDF file, 0.02 MB.

TABLE S4, XLSX file, 0.1 MB.

TABLE S5, XLS file, 3.7 MB.

ACKNOWLEDGMENTS

This work was supported by grants from the French National Research Agency (ANR-10-LABX-62-IBRID), and from the European Union's Horizon 2020 Research and Innovation Program under grant agreement no. 773830 (Project MedVetKlebs, One Health EJP). Adriana Chiarelli is part of the Pasteur-Paris University (PPU) International PhD Program, with funding from the Institut Carnot Pasteur Microbes & Santé, and the European Union's Horizon 2020 research and innovation program under the Marie Skłodowska-Curie grant agreement no. 665807.

We thank Rafael Patiño-Navarrete for his help in the bioinformatics analysis and Laurence Ma from the Institut Pasteur Biomics platform (C2RT, Institut Pasteur, Paris, France, supported by France Génomique, ANR-10-INBS-09-09 and IBISA) for her help in Illumina sequencing.

REFERENCES

- Wyres KL, Holt KE. 2018. *Klebsiella pneumoniae* as a key trafficker of drug resistance genes from environmental to clinically important bacteria. *Curr Opin Microbiol* 45:131–139. <https://doi.org/10.1016/j.mib.2018.04.004>.
- Navon-Venezia S, Kondratyeva K, Carattoli A. 2017. *Klebsiella pneumoniae*: a major worldwide source and shuttle for antibiotic resistance. *FEMS Microbiol Rev* 41:252–275. <https://doi.org/10.1093/femsre/fux013>.
- David S, Reuter S, Harris SR, Glasner C, Feltwell T, Argimon S, Abudahab K, Goater R, Giani T, Errico G, Aspbury M, Sjunnebo S, Feil EJ, Rossolini GM, Aanensen DM, Grundmann H. 2019. Epidemic of carbapenem-resistant *Klebsiella pneumoniae* in Europe is driven by nosocomial spread. *Nat Microbiol* 4:1919–1929. <https://doi.org/10.1038/s41564-019-0492-8>.
- Wyres KL, Hawkey J, Hetland MAK, Fostervold A, Wick RR, Judd LM, Hamidian M, Howden BP, Lohr IH, Holt KE. 2019. Emergence and rapid global dissemination of CTX-M-15-associated *Klebsiella pneumoniae* strain ST307. *J Antimicrob Chemother* 74:577–581. <https://doi.org/10.1093/jac/dky492>.
- Roe CC, Vazquez AJ, Esposito EP, Zarrilli R, Sahl JW. 2019. Diversity, virulence, and antimicrobial resistance in isolates from the newly emerging *Klebsiella pneumoniae* ST101 lineage. *Front Microbiol* 10:542. <https://doi.org/10.3389/fmicb.2019.00542>.
- Bonnin RA, Jousset AB, Chiarelli A, Emeraud C, Glaser P, Naas T, Dortet L. 2020. Emergence of new non-clonal group 258 high-risk clones among *Klebsiella pneumoniae* carbapenemase-producing *K. pneumoniae* isolates, France. *Emerg Infect Dis* 26:1212–1220. <https://doi.org/10.3201/eid2606.191517>.
- Tato M, Coque TM, Ruçz-Garbajosa P, Pintado V, Cobo J, Sader HS, Jones RN, Baquero F, Canton R. 2007. Complex clonal and plasmid epidemiology in the first outbreak of Enterobacteriaceae infection involving VIM-1 metallo-beta-lactamase in Spain: toward endemicity? *Clin Infect Dis* 45:1171–1178. <https://doi.org/10.1086/522288>.
- Tato M, Morosini M, Garcia L, Alberti S, Coque MT, Canton R. 2010. Carbapenem heteroresistance in VIM-1-producing *Klebsiella pneumoniae* isolates belonging to the same clone: consequences for routine susceptibility testing. *J Clin Microbiol* 48:4089–4093. <https://doi.org/10.1128/JCM.01130-10>.
- Snitkin ES, Zelazny AM, Thomas PJ, Stock F, Henderson DK, Palmore TN, Segre JA. 2012. Tracking a hospital outbreak of carbapenem-resistant *Klebsiella pneumoniae* with whole-genome sequencing. *Sci Transl Med* 4:148ra116. <https://doi.org/10.1126/scitranslmed.3004129>.
- Lazaro-Perona F, Sotillo A, Troyano-Hernaez P, Gomez-Gil R, de la Vega-Bueno A, Mingorance J. 2018. Genomic path to pandrug resistance in a clinical isolate of *Klebsiella pneumoniae*. *Int J Antimicrob Agents* 52:713–718. <https://doi.org/10.1016/j.ijantimicag.2018.08.012>.
- Sotillo A, Munoz-Velez M, Santamaria ML, Ruiz-Carrascoso G, Garcia-Bujalance S, Gomez-Gil R, Mingorance J. 2015. Emergence of VIM-1-producing *Salmonella enterica* serovar Typhimurium in a paediatric patient. *J Med Microbiol* 64:1541–1543. <https://doi.org/10.1099/jmm.0.000170>.
- Pérez-Vazquez M, Oteo-Iglesias J, Sola-Campoy PJ, Carrizo-Manzoni H, Bautista V, Lara N, Aracil B, Alhambra A, Martínez-Martínez L, Campos J, Sánchez-Romero I, Orden B, Martínez-Ruiz R, Aznar E, Cercenado E, de la Iglesia P, López-Urrutia L, Salso S, Vicente Saz J, Reyes S, Cobos J, García-Picazo L, Ortega-Lafont M, Megías-Lobón G, Andrés NA, Tarazona ER, Álvarez-García P, Fontanals D, Carranza R, Hernandez S, Fe Brezmes M, Ruiz-Velasco LM, Cascales P, Guerrero C, Yolanda G, Rodríguez-Conde I, Saez A. 2019. Characterization of carbapenemase-producing *Klebsiella oxytoca* in Spain. *Antimicrob Agents Chemother* 63:2016–2017. <https://doi.org/10.1128/AAC.02529-18>.
- Pérez-Viso B, Hernández-García M, Ponce-Alonso M, Morosini MI, Ruiz-Garbajosa P, Del Campo R, Cantón R. 2021. Characterization of carbapenemase-producing *Serratia marcescens* and whole-genome sequencing for plasmid typing in a hospital in Madrid, Spain (2016–18). *J Antimicrob Chemother* 76:110–116. <https://doi.org/10.1093/jac/dkaa398>.
- Poirel L, Bonnin RA, Nordmann P. 2012. Genetic features of the widespread plasmid coding for the carbapenemase OXA-48. *Antimicrob Agents Chemother* 56:559–562. <https://doi.org/10.1128/AAC.05289-11>.
- Nicolas-Chanoine MH, Mayer N, Guyot K, Dumont E, Pagès JM. 2018. Interplay between membrane permeability and enzymatic barrier leads to antibiotic-dependent resistance in *Klebsiella pneumoniae*. *Front Microbiol* 9:1422. <https://doi.org/10.3389/fmicb.2018.01422>.
- Hentschke M, Wolters M, Sobottka I, Rohde H, Aepfelbacher M. 2010. *ramR* mutations in clinical isolates of *Klebsiella pneumoniae* with reduced susceptibility to tigecycline. *Antimicrob Agents Chemother* 54:2720–2723. <https://doi.org/10.1128/AAC.00085-10>.
- Bialek-Davenet S, Lavigne JP, Guyot K, Mayer N, Tournebise R, Brisse S, Leflon-Guibout V, Nicolas-Chanoine MH. 2015. Differential contribution of AcrAB and OqxAB efflux pumps to multidrug resistance and virulence in *Klebsiella pneumoniae*. *J Antimicrob Chemother* 70:81–88. <https://doi.org/10.1093/jac/dku340>.
- Wan Nur Ismah WAK, Takebayashi Y, Findlay J, Heesom KJ, Avison MB. 2018. Impact of OqXR loss of function on the envelope proteome of *Klebsiella pneumoniae* and susceptibility to antimicrobials. *J Antimicrob Chemother* 73:2990–2996. <https://doi.org/10.1093/jac/dky293>.
- Baker S, Hardy J, Sanderson KE, Quail M, Goodhead I, Kingsley RA, Parkhill J, Stocker B, Dougan G. 2007. A novel linear plasmid mediates flagellar variation in *Salmonella Typhi*. *PLoS Pathog* 3:e59. <https://doi.org/10.1371/journal.ppat.0030059>.
- Candales MA, Duong A, Hood KS, Li T, Neufeld RA, Sun R, McNeil BA, Wu L, Jarding AM, Zimmerly S. 2012. Database for bacterial group II introns. *Nucleic Acids Res* 40:D187–D190. <https://doi.org/10.1093/nar/gkr1043>.
- Partridge SR, Hall RM. 2003. The IS1111 family members IS4321 and IS5075 have subterminal inverted repeats and target the terminal inverted repeats of Tn21 family transposons. *J Bacteriol* 185:6371–6384. <https://doi.org/10.1128/jb.185.21.6371-6384.2003>.
- Nicolas E, Lambin M, Dandoy D, Galloy C, Nguyen N, Oger CA, Hallet B. 2015. The Tn3-family of replicative transposons. *Microbiol Spectr* 3(4):MDNA3-0060-2014. <https://doi.org/10.1128/microbiolspec.MDNA3-0060-2014>.
- Farmer JJ, III, Davis BR, Hickman-Brenner FW, McWhorter A, Huntley-Carter GP, Asbury MA, Riddle C, Wathen-Grady HG, Elias C, Fanning GR. 1985. Biochemical identification of new species and biogroups of Enterobacteriaceae isolated from clinical specimens. *J Clin Microbiol* 21:46–76. <https://doi.org/10.1128/JCM.21.1.46-76.1985>.
- Wyres KL, Holt KE. 2016. *Klebsiella pneumoniae* population genomics and antimicrobial-resistant clones. *Trends Microbiol* 24:944–956. <https://doi.org/10.1016/j.tim.2016.09.007>.
- Quainoo S, Coolen JPM, van Hijum S, Huynen MA, Melchers WJG, van Schaik W, Wertheim HFL. 2017. Whole-genome sequencing of bacterial pathogens: the future of nosocomial outbreak analysis. *Clin Microbiol Rev* 30:1015–1063. <https://doi.org/10.1128/CMR.00016-17>.
- Jousset AB, Bonnin RA, Rosinski-Chupin I, Girlich D, Cuzon G, Cabanel N, Frech H, Farfour E, Dortet L, Glaser P, Naas T. 2018. A 4.5-year within-patient evolution of a colistin-resistant *Klebsiella pneumoniae* carbapenemase-producing *K. pneumoniae* sequence type 258. *Clin Infect Dis* 67:1388–1394. <https://doi.org/10.1093/cid/ciy293>.
- Mathers AJ, Stoesser N, Sheppard AE, Pankhurst L, Giess A, Yeh AJ, Didelot X, Turner SD, Sebra R, Kasarskis A, Peto T, Crook D, Sifri CD. 2015. *Klebsiella pneumoniae* carbapenemase (KPC)-producing *K. pneumoniae* at a single institution: insights into endemicity from whole-genome sequencing. *Antimicrob Agents Chemother* 59:1656–1663. <https://doi.org/10.1128/AAC.04292-14>.
- Stoesser N, Giess A, Batty EM, Sheppard AE, Walker AS, Wilson DJ, Didelot X, Bashir A, Sebra R, Kasarskis A, Sthapit B, Shakya M, Kelly D, Pollard AJ, Peto TE, Crook DW, Donnelly P, Thorson S, Amatya P, Joshi S. 2014. Genome sequencing of an extended series of NDM-producing *Klebsiella pneumoniae* isolates from neonatal infections in a Nepali hospital characterizes the extent of community- versus hospital-associated transmission in an endemic setting. *Antimicrob Agents Chemother* 58:7347–7357. <https://doi.org/10.1128/AAC.03900-14>.
- Santos-Lopez A, Marshall CW, Scribner MR, Snyder DJ, Cooper VS. 2019. Evolutionary pathways to antibiotic resistance are dependent upon environmental structure and bacterial lifestyle. *Elife* 8:e47612. <https://doi.org/10.7554/eLife.47612>.
- Pitart C, Solé M, Roca I, Fàbrega A, Vila J, Marco F. 2011. First outbreak of a plasmid-mediated carbapenem-hydrolyzing OXA-48 beta-lactamase in *Klebsiella pneumoniae* in Spain. *Antimicrob Agents Chemother* 55:4398–4401. <https://doi.org/10.1128/AAC.00329-11>.
- Matsumura Y, Peirano G, Bradford PA, Motyl MR, DeVinney R, Pitout JDD. 2018. Genomic characterization of IMP and VIM carbapenemase-encoding transferable plasmids of Enterobacteriaceae. *J Antimicrob Chemother* 73:3034–3038. <https://doi.org/10.1093/jac/dky303>.
- Rutherford JC. 2014. The emerging role of urease as a general microbial virulence factor. *PLoS Pathog* 10:e1004062. <https://doi.org/10.1371/journal.ppat.1004062>.
- Eaton KA, Brooks CL, Morgan DR, Krakowka S. 1991. Essential role of urease in pathogenesis of gastritis induced by *Helicobacter pylori* in gnotobiotic piglets. *Infect Immun* 59:2470–2475. <https://doi.org/10.1128/IAI.59.7.2470-2475.1991>.

34. De Koning-Ward TF, Robins-Browne RM. 1995. Contribution of urease to acid tolerance in *Yersinia enterocolitica*. *Infect Immun* 63:3790–3795. <https://doi.org/10.1128/IAI.63.10.3790-3795.1995>.
35. Rózalski A, Sidorczyk Z, Kotelko K. 1997. Potential virulence factors of *Proteus* bacilli. *Microbiol Mol Biol Rev* 61:65–89. <https://doi.org/10.1128/61.1.65-89.1997>.
36. Benoit SL, Schmalstig AA, Glushka J, Maier SE, Edison AS, Maier RJ. 2019. Nickel chelation therapy as an approach to combat multi-drug resistant enteric pathogens. *Sci Rep* 9:13851. <https://doi.org/10.1038/s41598-019-50027-0>.
37. Maroncle N, Rich C, Forestier C. 2006. The role of *Klebsiella pneumoniae* urease in intestinal colonization and resistance to gastrointestinal stress. *Res Microbiol* 157:184–193. <https://doi.org/10.1016/j.resmic.2005.06.006>.
38. Gorrie CL, Mirceta M, Wick RR, Judd LM, Wyres KL, Thomson NR, Strugnell RA, Pratt NF, Garlick JS, Watson KM, Hunter PC, McGloughlin SA, Spelman DW, Jenney AWJ, Holt KE. 2018. Antimicrobial-resistant *Klebsiella pneumoniae* carriage and infection in specialized geriatric care wards linked to acquisition in the referring hospital. *Clin Infect Dis* 67:161–170. <https://doi.org/10.1093/cid/ciy027>.
39. Clinical and Laboratory Standards Institute (CLSI). 2016. Performance standards for antimicrobial susceptibility testing, twenty-seventh informational supplement, M100-S25 edition. Clinical and Laboratory Standards Institute, Wayne, PA.
40. Bankevich A, Nurk S, Antipov D, Gurevich AA, Dvorkin M, Kulikov AS, Lesin VM, Nikolenko SI, Pham S, Pribelski AD, Pyshkin AV, Sirotkin AV, Vyahhi N, Tesler G, Alekseyev MA, Pevzner PA. 2012. SPAdes: a new genome assembly algorithm and its applications to single-cell sequencing. *J Comput Biol* 19:455–477. <https://doi.org/10.1089/cmb.2012.0021>.
41. Chin CS, Alexander DH, Marks P, Klammer AA, Drake J, Heiner C, Clum A, Copeland A, Huddleston J, Eichler EE, Turner SW, Korlach J. 2013. Nonhybrid, finished microbial genome assemblies from long-read SMRT sequencing data. *Nat Methods* 10:563–569. <https://doi.org/10.1038/nmeth.2474>.
42. Koren S, Walenz BP, Berlin K, Miller JR, Bergman NH, Phillippy AM. 2017. Canu: scalable and accurate long-read assembly via adaptive k-mer weighting and repeat separation. *Genome Res* 27:722–736. <https://doi.org/10.1101/gr.215087.116>.
43. Deatherage DE, Barrick JE. 2014. Identification of mutations in laboratory-evolved microbes from next-generation sequencing data using breseq. *Methods Mol Biol* 1151:165–188. https://doi.org/10.1007/978-1-4939-0554-6_12.
44. Seemann T. 2014. Prokka: rapid prokaryotic genome annotation. *Bioinformatics* 30:2068–2069. <https://doi.org/10.1093/bioinformatics/btu153>.
45. Wyres KL, Nguyen TNT, Lam MMC, Judd LM, van Vinh Chau N, Dance DAB, Ip M, Karkey A, Ling CL, Miliya T, Newton PN, Lan NPH, Sengduangphachanh A, Turner P, Veeraraghavan B, Vinh PV, Vongsouvath M, Thomson NR, Baker S, Holt KE. 2020. Genomic surveillance for hypervirulence and multi-drug resistance in invasive *Klebsiella pneumoniae* from South and Southeast Asia. *Genome Med* 12:11. <https://doi.org/10.1186/s13073-019-0706-y>.
46. Bortolaia V, Kaas RS, Ruppe E, Roberts MC, Schwarz S, Cattoir V, Philippon A, Allesoe RL, Rebelo AR, Florensa AF, Fagelhauer L, Chakraborty T, Neumann B, Werner G, Bender JK, Stingl K, Nguyen M, Coppens J, Xavier BB, Malhotra-Kumar S, Westh H, Pinholt M, Anjum MF, Duggett NA, Kempf I, Nykäsenoja S, Olkkola S, Wiczorek K, Amaro A, Clemente L, Mossong J, Losch S, Ragimbeau C, Lund O, Aarestrup FM. 2020. ResFinder 4.0 for predictions of phenotypes from genotypes. *J Antimicrob Chemother* 75:3491–3500. <https://doi.org/10.1093/jac/dkaa345>.
47. Carattoli A, Zankari E, Garcia-Fernandez A, Voldby Larsen M, Lund O, Villa L, Moller Aarestrup F, Hasman H. 2014. In silico detection and typing of plasmids using PlasmidFinder and plasmid multilocus sequence typing. *Antimicrob Agents Chemother* 58:3895–3903. <https://doi.org/10.1128/AAC.02412-14>.
48. Almeida A, Villain A, Joubrel C, Touak G, Sauvage E, Rosinski-Chupin I, Poyart C, Glaser P. 2015. Whole-genome comparison uncovers genomic mutations between group B streptococci sampled from infected newborns and their mothers. *J Bacteriol* 197:3354–3366. <https://doi.org/10.1128/JB.00429-15>.
49. Sayers EW, Karsch-Mizrachi I. 2016. Using GenBank. *Methods Mol Biol* 1374:1–22. https://doi.org/10.1007/978-1-4939-3167-5_1.
50. Treangen TJ, Ondov BD, Koren S, Phillippy AM. 2014. The Harvest suite for rapid core-genome alignment and visualization of thousands of intraspecific microbial genomes. *Genome Biol* 15:524. <https://doi.org/10.1186/s13059-014-0524-x>.
51. Letunic I, Bork P. 2019. Interactive Tree Of Life (iTOL) v4: recent updates and new developments. *Nucleic Acids Res* 47:W256–W259. <https://doi.org/10.1093/nar/gkz239>.
52. O'Toole GA, Kolter R. 1998. Initiation of biofilm formation in *Pseudomonas fluorescens* WCS365 proceeds via multiple, convergent signalling pathways: a genetic analysis. *Mol Microbiol* 28:449–461. <https://doi.org/10.1046/j.1365-2958.1998.00797.x>.
53. Favre-Bonte S, Joly B, Forestier C. 1999. Consequences of reduction of *Klebsiella pneumoniae* capsule expression on interactions of this bacterium with epithelial cells. *Infect Immun* 67:554–561. <https://doi.org/10.1128/IAI.67.2.554-561.1999>.